PCCP

Accepted Manuscript

ROYAL SOCIETY OF CHEMISTRY

www.rsc.org/pccp

A unified study for water adsorption on metals: meaningful models from structural motifs

Guillem Revilla-López,* Núria López*

Institute of Chemical Research of Catalonia, ICIQ, Av. Països Catalans 16, 43007 Tarragona, Spain; nlopez@iciq.es

The adsorption of the first water layer on metals combines several structural motifs like pentagons, hexagons, and heptagons interconnected variably leading to a myriad of patterns. Although theoretical methods are now able to discriminate the ground states, there is a need to find simple ways to account for the relative stability of different patterns on the surface. Taking the already reported structures for water bilayers as training sets we have decomposed the adsorption energy of each of the motifs to their fundamental components: water-water and water-metal interactions through strain-induced surface metal deformations. Models coming from this scheme can be used to survey the properties of many of the structures reported irrespectively of their complexity, thus providing a simple structure-based tool to assess likeliness, relative stability, wettability, and main patterns of water motifs on metals.

1.Introduction

Water forms a thin layer on most of the surfaces exposed to atmospheric conditions.[1-3] This aqueous coating is involved in many physical, chemical, technological and environmental phenomena such as corrosion, heterogeneous catalysis, electro- and photochemistry and ice nucleation.[4] The elucidation of interactions between water and surfaces at the atomic scale is crucial for a complete understanding of these processes. Huge efforts have been made to study the first wetting layer and its three-dimensional growth, particularly on metals.[1-3,5-10] A recent review[1] has identified the remaining challenges: the structure of the lowest energy interfacial layer and the derivation of physically meaningful models to estimate the adsorption energy of each ensemble on a transition metal surface. The delicate balance between water-water and water-metal interactions has been reported by Michaelides[5-7] *et al.* and Salmeron[8] *et al.* to rule the adsorption of water forming motifs.

Our aim goes beyond the classical qualitative view of the balance between the two components leading water adsorption. The main goal of this work is to assign the water-water and water-metal interactions to precise variables in order to build models able to predict the adsorption energy of a given water ensemble. Such models, based on the structural motifs, must provide a first reliable energy estimate of different metastable structures. To this end, we used three main groups of structures: not linked clusters, hexagon-only two-dimensional arrays, pentagon-hexagon-heptagon layers, that are extensively documented in the literature.[1,3] Density Functional Theory based calculations with dispersion contributions were employed to obtain the adsorption of the different motifs on Pd, Pt, and Ru. As strain-induced deformations of the metal surface and the subjacent metal bulk layers modifies the water-metal (through alteration of the metal *d*-states energy[11,12]) and water-water interactions to different extents, *xy* plane distortions is the sole tool that allows to disentangle these contributions to the total adsorption energy. Besides, there has been a steady claim for models establishing a unified model able to assess the relative stability range of different potential ground states. [1]

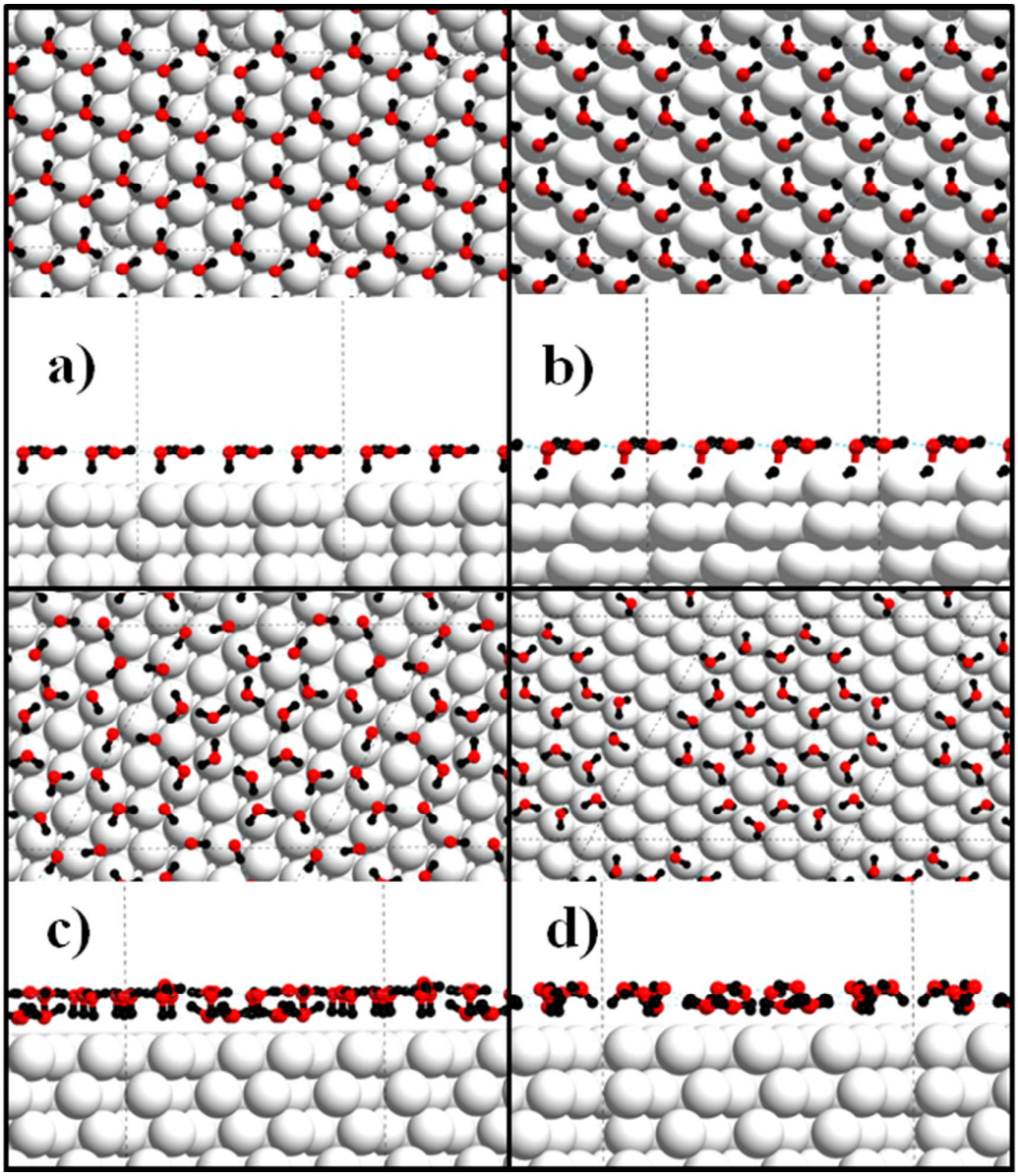

Figure 1: Axial and longitudinal views of the water structures on fcc (111) or equivalent hcp (0001) facets of: a) molecular H-down Ice-like layer, b) dissociated Ice-like layer, c) sqrt(37), d) Rosette. Metal, oxygen, and hydrogen atoms represented by grey, red, and black spheres respectively.

Pd, Pt, and Ru are the three metal surfaces for which most structural information of the water-metal interfaces has been gathered.[3] The lattice parameters of the lowest energy facets (111) or (0001) are roughly $\sqrt{3}$ times the value for ice bulk. Initial models proposed a rotated Ice-like bilayer structure ($\sqrt{3}x\sqrt{3} - R30^o$) with a coverage of 0.67 ML,[1] Figure 1. Feibelman and co-workers,[13] in a combined STM-DFT study on Pt(111) identified a continuous structure with pentagons, hexagons, and heptagons in a $\sqrt{37}x\sqrt{37} - R\ 25.3°$ arrangement, hereafter sqrt(37), though H-down Ice-like bilayer was also found to be metastable.[14] This sqrt(37) bilayer, contained a rotated hexameric cycle made of flat lying waters in the center with 0.70 ML coverage. Other structures with the same patterns, like $\sqrt{39}x\sqrt{39} - R\ 16.1°$, present a different rotation of the central hexagon, a coverage of 0.69 ML, and are metastable between 130 and 140 K.[15] For Pd(111), adsorption experiments in the sub-monolayer coverage regime (0.5 ML) identified two patterns: Rosette and Lace.[16] While Rosettes behave as "magic clusters" and are isolated on the surface Figure 1, Laces exhibit a pattern of chained six water membered rings that extends over all the surface. Reactive metal surfaces like Ru(0001) add complexity, as they partially dissociate water above 150 K, Figure 1.b and caption, creating a structure that retains the ice honeycomb pattern but with low buckling.[3] The exact amount of dissociated waters is under discussion due to the fact that experiments use variable temperature[17] or deuterium isotopes[18] which can have strong effects on the dissociation rate. For simplicity, only the 50% dissociated model has been considered.

2.Methods

Slabs under periodic boundary conditions are used to represent the metal close-packed (111) surfaces of Pd, Pt, Ag, Au, Ir, and Rh and the equivalent Ru(0001). Energies were obtained through Density Functional Theory (DFT) calculations carried out with the Vienna Ab-initio Simulation Package (VASP).[19] Unless explicitly stated, all energies reported in figures and tables or obtained through equations are expressed in eV/H_2O. In VASP, the electron−ion interaction is described within the projector-augmented-wave formalism[20,21] and the monoelectronic valence state by plane-waves with kinetic energies up to 450 eV. The PBE[22] functional was used. Dispersion contributions were included through the simplified Grimme formalism with the parameters adapted for metals.[23-25] With this setup the cohesive energy per water molecule in bulk ice is -0.764 eV/H_2O. In comparison, the average interaction energies

are -0.454, -0.296, -0.221 eV/H_2O, for the standing Ice-like bilayer, sqrt(37), and Rosette water ensembles, respectively.

Water adsorption was considered at different coverages: Rosette (0.50 ML, water molecules *w*=24, surface metal atoms *s*=48), a three-fold enlarged H-down Ice-like bilayer ($3\sqrt{3}x3\sqrt{3}-R30^{o}$, 0.67 ML, *w*=18, *s*=27) to minimize differences with small unit cells, and sqrt(37) (0.70 ML *w*=26, *s*=37) and Rosette. For Ru, both the molecular and the 50% dissociated models of the Ice-like bilayer structure were considered. For the fcc (hcp) metals, a four (five) layer metal slab was interleaved by a vacuum space of ~16 Å. The Brillouin zone was sampled using 3×3×1 (large cells) Γ-centered k-point mesh. Convergence tests are presented in Figure S1 and its caption. Deformations within ±10% in the *xy* plane (d_{XY}) were considered, in line with refs. [11,12]. These percentages are considered with regard the unstrained inter-metal distance in the undeformed slab and are applied to both the metal surface and the bulk-like three (four for Ru) layers lying immediately below it. Expansions and contractions in the *xy* plane of the metal slab increase and decrease the *d*-states energeies in a linear way[11,12] respectively and, consequently, the energy of their hybridization with the lone pair electrons from water oxygens (water monomer adsorption energy) stabilizes linearly with expansions and vice versa with contractions, as demonstrated for CO,[11] O[11,12] and H.[12] Adsorption energies under deformations (±4%) were used to develop the models, see Figure 2 and its caption. The large flexibility of the web of interactions in water ensures that bilayers are maintained when strain is introduced and only adsorption energies are affected. Electronic convergence was set to 10^{-5} eV and atomic convergence used a 15 meV/Å threshold for the forces on the adsorbates.

The present energies correspond to 0 K temperatures. The effect of the temperature in the absolute adsorption energies and the different stability of the motifs is two-fold: (i) from the gas-phase the absolute adsorption energies would be reduced, (ii) very ordered structures would be less stable than the labile ones.

3.Results and discussion

3.1 Strain effects on DFT adsorption energies

The DFT-D2 adsorption energies for the different set of training structures under ±4% d_{XY} deformation are presented in Table 1 in eV·H_2O^{-1}. Table 2 also reports adsorption energies but in eV·$Å^{-2}$ to better adjust to experimental results. From a direct

comparison of values in Table1 and Table 2 we can check that the adsorption energies show an inverse pattern. The reason lies in the different coverages by which adsorption energy is normalized. In this case, magic clusters like Rosette that has considerably exothermic adsorption energies but low coverage, 0.5 ML, results the most stable. On the other hand, sqrt(37) with the most exothermic adsorption energy per water monomer is found to shift to the second position of the ranking due to its relative high coverage, 0.70 ML. Ice-like is an intermediate case in terms of coverage, 0.67 ML, and the least stable in terms of energy per molecule. Thus it remains in the third position in the stability ranking with no so big changes like in the two previous cases.

Table 1: (a) DFT-D2 calculated adsorption energies for H-down Ice-like, sqrt(37) and Rosette structures on Pd, Pt and Ru. All energies are in eV/H_2O. All d_{XY} are in plane deformation (in %) with respect to the unstrained metal slab.

	Pd(111)			Pt(111)			Ru(0001)			
d_{XY}	Ice-like	sqrt(37)	Rosette	Ice-like	sqrt(37)	Rosette	Ice-like	Ice-like Diss.	sqrt(37)	Rosette
4	-0.621	-0.706	-0.669	-0.603	-0.693	-0.667	-0.601	-0.971	-0.780	-0.777
2	-0.627	-0.708	-0.663	-0.604	-0.696	-0.655	-0.617	-0.952	-0.754	-0.761
0	-0.631	-0.703	-0.663	-0.611	-0.696	-0.642	-0.610	-0.870	-0.747	-0.737
-2	-0.632	-0.700	-0.663	-0.616	-0.692	-0.628	-0.592	-0.779	-0.736	-0.703
-4	-0.629	-0.694	-0.636	-0.615	-0.684	-0.614	-0.603	-0.678	-0.718	-0.678

Table 2: (a) DFT-D2 calculated adsorption energies for H-down Ice-like, sqrt(37) and Rosette structures on Pd, Pt and Ru. All energies are in eV/$Å^{-2}$. All d_{XY} are in plane deformation (in %) with respect to the unstrained metal slab.

	Pd(111)			Pt(111)			Ru(0001)			
d_{XY}	Ice-like	sqrt(37)	Rosette	Ice-like	sqrt(37)	Rosette	Ice-like	Ice-like Diss.	sqrt(37)	Rosette
4	-0.239	-0.260	-0.345	-0.232	-0.255	-0.344	-0.231	-0.358	-0.402	-0.401
2	-0.241	-0.261	-0.342	-0.232	-0.256	-0.338	-0.237	-0.351	-0.389	-0.392
0	-0.243	-0.259	-0.342	-0.235	-0.256	-0.331	-0.235	-0.320	-0.385	-0.380
-2	-0.243	-0.258	-0.342	-0.237	-0.255	-0.324	-0.228	-0.287	-0.379	-0.362
-4	-0.242	-0.256	-0.328	-0.237	-0.252	-0.316	-0.232	-0.250	-0.370	-0.349

For unstrained Pd(111), the adsorption energies reveal a thermodynamic preference for sqrt(37), -0.703 eV/H_2O, Rosette and the Ice-like bilayer being less stable, -0.663, -0.631 eV/H_2O, respectively. The cohesive energy of bulk hexagonal ice is more exothermic than the previous values: -0.764 eV/H_2O. However, objections must be made about comparisons of this value with the adsorption energies of the motifs on metal surfaces: (*i*) inter-motif thermodynamic stability comparison is possible based on their ground state energy without regard of the ice cohesive energy, (*ii*) coverage employed in both calculations and experiments prevents multi-layer growth thus ice cohesive energy is not directly comparable to adsorption energy, (*iii*) Adsorption energies are always higher than standing Ice-like bilayer. The latter statement points to the stabilizing effect of the adsorption on metals for these motifs. For Pt(111), the adsorption energies are -0.696, -0.642 and -0.611 eV/H_2O, respectively. On Ru(0001)[5,26-29] the H-down water molecules can dissociate but this is not possible for either sqrt(37) and Rosette structures, as the water molecules close to the surface are only in flat configurations. Consequently, dissociated Ice-like bilayer is thermodynamically preferred, -0.870 eV/H_2O, followed by sqrt(37), Rosette and molecular ice: -0.747, -0.737 and -0.610 eV/H_2O, respectively. By applying deformations the thermodynamic ordering for the ensembles is maintained (Figure 2 and caption). The adsorption energies become larger as extensive strains are applied. However, there is no unified effect of strain on all the ensembles. Some present a minimum well like the Ice-like bilayer on Pd(111), while others show a linear dependence. Examples of the later are the Rosette structures in Pt(111). A remarkable difference is found for Ru(0001): the adsorption energy of the different ensembles degenerates under 4% compression.

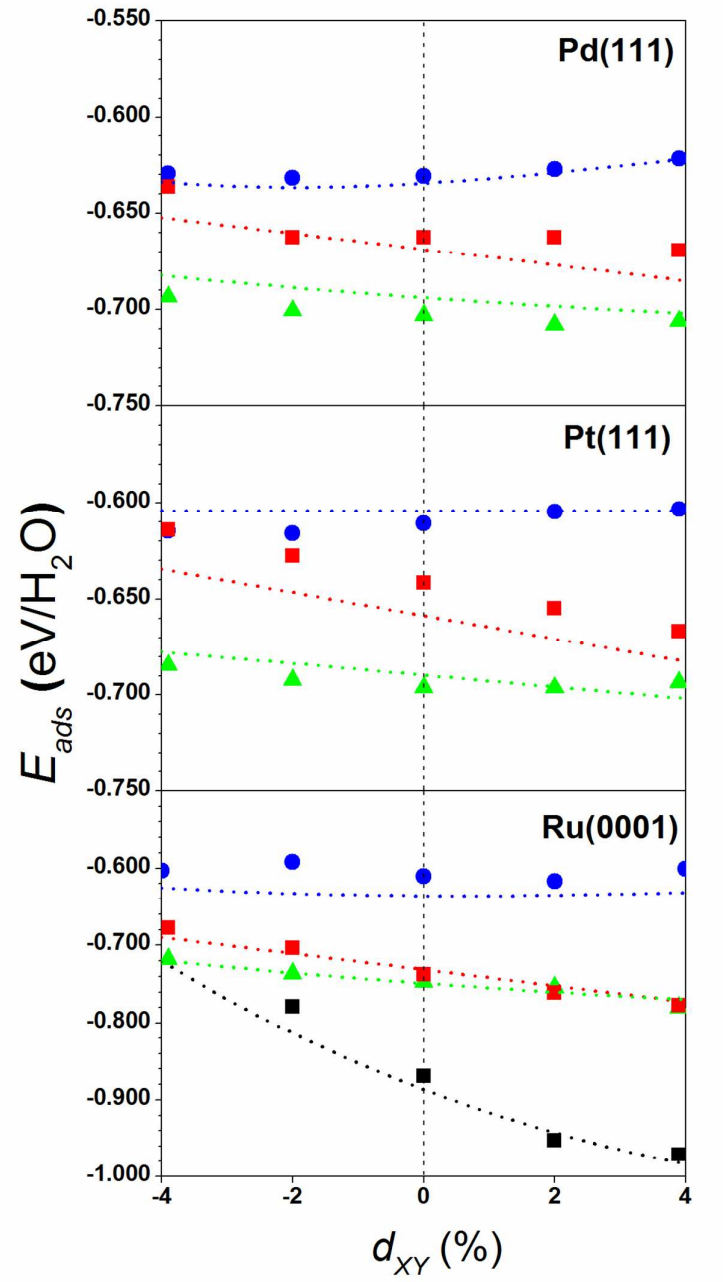

Figure 2: DFT-D2 calculated adsorption energies, E_{ads} eV/H_2O, for the metals and the three water ensembles at different deformation degrees (±4%) with regard to the equilibrium d_{XY}=0: Ice-like bilayer (blue squares), half-dissociated Ice-like bilayer (black squares), sqrt(37) (green triangles) and Rosette (red circles). The dashed lines which follow the same color code represent the adsorption energies for the three ensembles modeled with Eqs. (1-3).

3.2. Driving factors of water motif adsorption

Based on the DFT-energies we have put forward the energy decomposition of the adsorption energy of the ensembles in terms of the two main components: the water-metal, $E_{M,d}^{w}$, and the water-water interactions once the metal effects are subtracted. $E_{M,d}^{w}$ is analyzed through the adsorption energy of an isolated water molecule on a strained *p*(2x2) supercell of the corresponding metal, *M*. When two minima, flat and vertical, exist, like on Ru(0001), $E_{M,d}^{w}$ corresponds to the average, values are presented in Table S1. The differential behavior between Ru and the other metals is caused by the stronger hydrogen-metal bond in Ru than in Pd and Pt. The latter interaction eases water dissociation on Ru(0001).[14] $E_{M,d}^{w}$ contains the changes in water-metal interaction induced by the geometric distortion, d_{XY}, and these changes are explained by the linear variation of the *d*-states with the expansion,[11,12] see Figure 3 and its caption. Different slopes are found for the different metal: this metal-dependent linear behavior is explained through the interaction between distorted *d*-states and the lone pair electrons around oxygen.[11,12]

The water-water term contains two different contributions for the adsorbate layer: the first corresponds to the energy per hydrogen bond and it is strain-independent E_{HB}=-0.25 eV (Figure 3 and caption); the second contribution is the cooperative stabilization caused by the formation of 2D hydrogen bonding network and is the ice lattice resonance energy, $E_{res,d}^{ice}$. The latter energy does not consider the effect of the metal on water, nor does the former magnitude, but the stability that the honeycomb-like structure of ice induces once the energies of water monomers and individual hydrogen bonds are subtracted: $E_{res,d}^{ice} = (E_{d}^{ice} - n_w \cdot E_w - n_{HB} \cdot E_{HB})/n_w$, where E_{d}^{ice} represents the single point energy calculation of the lattice under a certain strain, E^w is the gas-phase isolated water energy and n_w and n_{HB} are the total number of water molecules and hydrogen bonds in the ensemble. Figure 3 shows the quadratic dependence of ice resonance energy with d_{XY} due to variations in distances between hydrogen bond donors and acceptors in both directions.

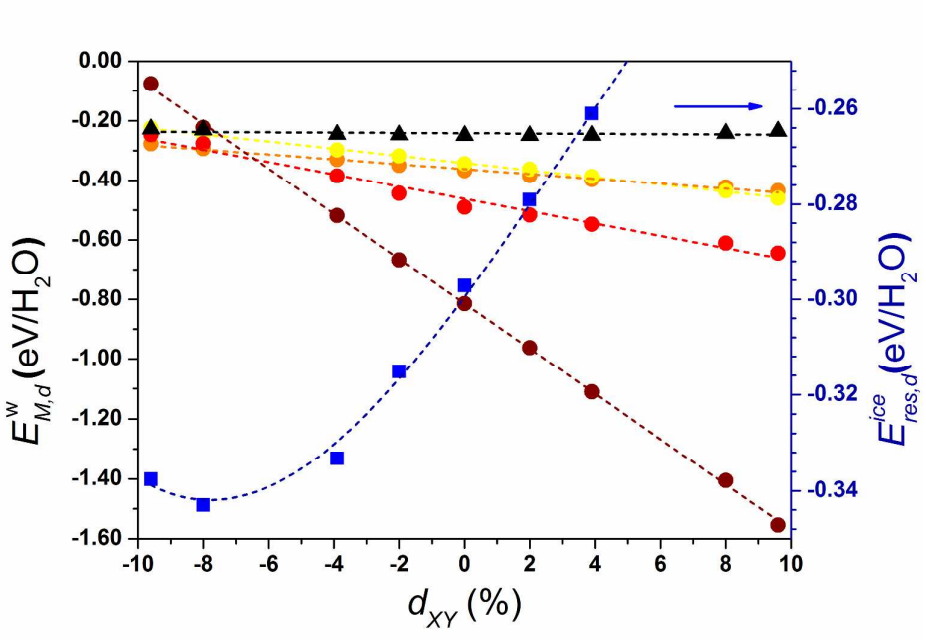

Figure 3: Energy factors governing water adsorption as a function of deformation, d_{XY}. Hydrogen bond E_{HB}=-0.25 calculated by distorting the dimer (black triangles and line). Circles represent water monomer adsorptions, $E^{w}_{M,d}$ in eV/H_2O: for Pd(111): $E^{w}_{Pd,d}$=-0.29d_{XY}+0.43, (orange); Pt(111): $E^{w}_{Pt,d}$=-0.42d_{XY}+0.83, (yellow); undissociated water on Ru(0001): $E^{w}_{Ru,d}$=-0.75d_{XY}+1.56 (red) and dissociated $E^{w-dis}_{Ru,d}$=-2.73d_{XY}+6.58, (wine). Ice resonance energy (use blue scale in the right) with a dependence on d_{XY} E^{ice}_{res} =1.34d_{XY}^2-6.9d_{XY}+8.5, in blue squares. Regression correlations coefficients can be found in Table 3.

Table 3. Polynomial parameters: α, β, γ with the corresponding errors and units in $eV \cdot H_2O^{-1} \cdot Å^{-2}$, $eV \cdot H_2O^{-1} \cdot Å^{-1}$ and $eV \cdot H_2O^{-1}$ respectively. Parameters are obtained from the regressions of isolated water adsorption on the different metals: $E^{w}_{M,d}$ on Pt(111), Pd(111), Ru(0001) including dissociated state for the adsorption on Ru. Resonance energy for the two dimensional ice layer $E^{ice}_{res,d}$ and hydrogen bond for the water dimer, E_{HB}. All these parameters take the functional dependence on the elongation d_{XY}: $E = \alpha d_{XY}^2 + \beta d_{XY} + \gamma$. The regression coefficient, r^2, is also presented.

	α	β	γ	r^2
$E^{w}_{Pd,d}$	-	-0.29±0.01	0.43±0.02	0.98
$E^{w}_{Pt,d}$	-	-0.42±0.01	0.83±0.01	0.98
$E^{w}_{Ru,d}$	-	-0.75±0.03	1.56±0.10	0.98
$E^{w,d}_{Ru,d}$	-	-2.73±0.00	6.58±0.00	1.00
$E^{ice}_{res,d}$	1.34±0.08	6.90±0.40	8.50±0.50	0.98
E_{HB}	-	-	0.25±0.00	1.00

4. Discussion

4.1 Adsorption energy model development

Under soft deformations (±4%) all the points of a same water structure family; H-down Ice-like bilayer, sqrt(37), and Rosettes, belong to different planes when correlated to water-metal and water-water interactions (Figure 4 and its caption). These correlations reveal the contributions of $E^{w}_{M,d}$ and $E^{ice}_{res,d}$ to Ice-like bilayer and sqrt(37) adsorption and the dependence of Rosette solely on $E^{w}_{M,d}$. In the following, adsorption energy models are explained.

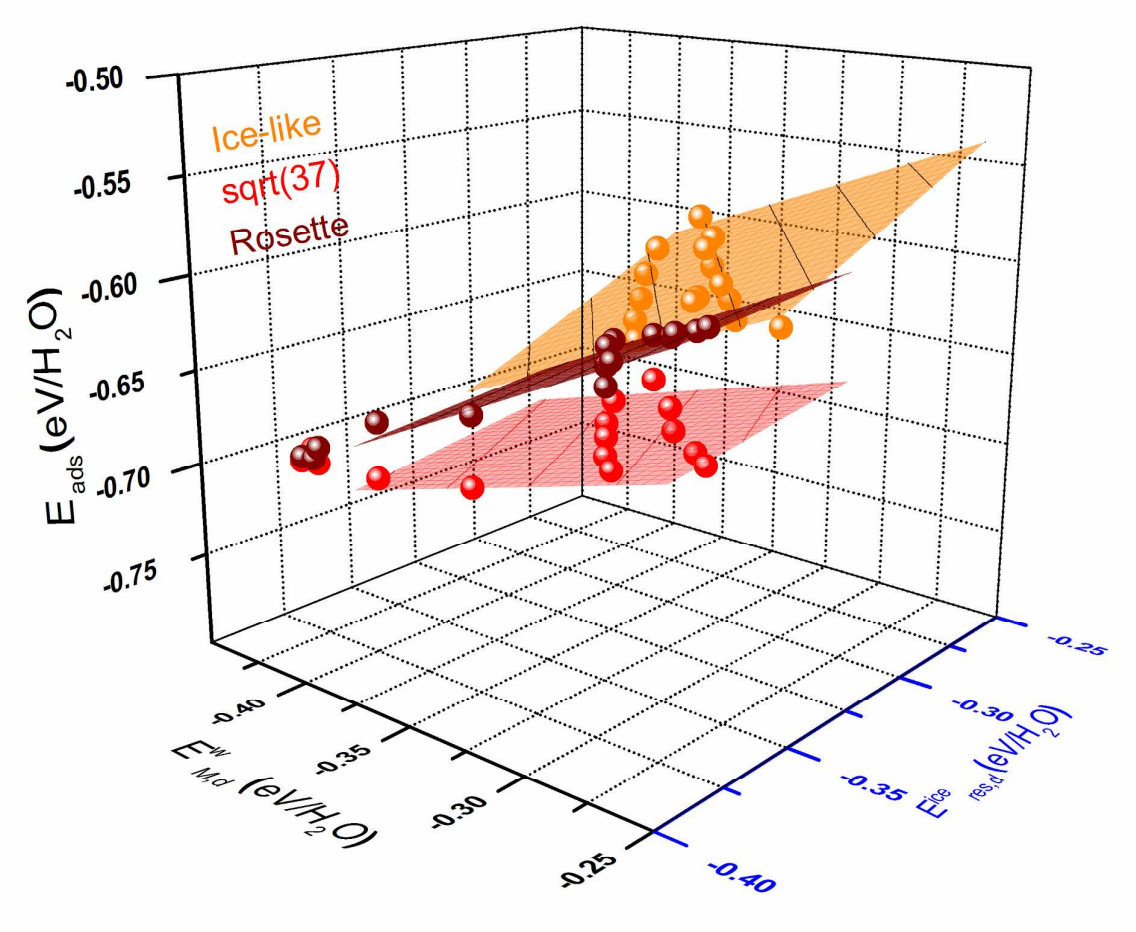

Figure 4: DFT-D2 adsorption energy, E_{ads}, as a function of the single water adsorption energy, $E_{M,d}^{w}$ and ice resonance energy, $E_{res,d}^{ice}$. The planes correspond to Equations (1-3). The correlation coefficients are 0.92, 0.97, and 0.96 for Eq(1-3), respectively.

The coefficients of the planes in Figure 4 render the models discussed in the following lines. Ice-like bilayer adsorption (in eV/H_2O) follows:

$$E_{ads}^{ice} = 1/2 \cdot E_{M,d}^{w} + 2/3 \cdot E_{res,d}^{ice} + E_{HB} \qquad \text{Eq. (1)}$$

The 50% contribution for $E_{M,d}^{w}$ reflects that only half of the water molecules fully interact with the metal; the $2/3$ for $E_{res,d}^{ice}$ stands for a dimensionality factor between induced deformation in the *xy* plane but not in the *z* direction and the three-dimensional nature of the bilayer. The last term, E_{HB}, is the remaining constant that corresponds to the stabilization of a hydrogen bond. Eq. (1) explains the flat response on Pt(111) when compared to the other two metals by a combination between linear

$E^{w}_{M,d}$ and quadratic $E^{ice}_{res,d}$. The model reproduces DFT energies adsorption energies with an average absolute error below 5%

The adsorption of the sqrt(37) in eV/H_2O follows:

$$E^{sqrt(37)}_{ads} = 9/26 \cdot E^{w}_{M,d} + 6/26 \cdot E^{ice}_{res,d} + 2E_{HB} \qquad \text{Eq. (2)}$$

The coefficient modulating $E^{ice}_{res,d}$ stands for the 6 metal interacting flat waters in the central cycle reminding that of ice, thus being the only ones affected by ice resonance. To explain the coefficient for $E^{w}_{M,d}$ it is necessary to take into account these central fully interacting waters plus six monomers which only interact partly thus the prefactor corresponds to 6/26+3/26. The equation above establishes a link between the energy representations of sqrt(37) and Ice-like bilayer and follows the conceptual works that relate sqrt(37) to a reorganization of Ice-like bilayer upon withdrawal of four water monomers.[13,30] The maximum absolute error of the model is ~2 %.

The sqrt(39) structure is an alternative structure for Pt[15] which can be used to assess the validity of the model, see structure in Figure 5. This motif presents presents the same combination of multi-membered cycles but totalling 27 water molecules. This renders smaller $E^{w}_{M,d}$ and $E^{ice}_{res,d}$ than in the sqrt(37) so the total contribution is less favorable for sqrt(39) which corroborates the higher stability of sqrt(37) found in experiments. [15]

Finally, the Rosette adsorption (in eV/H_2O)model is:

$$E^{ros}_{ads} = 12/24 \cdot E^{w}_{M,d} + 2E_{HB} \qquad \text{Eq. (3)}$$

Rosette adsorption is only dependent on $E^{w}_{M,d}$ plus the energy of two hydrogen bonds. The absence of a continuous hydrogen network fully covering the surface cancels $E^{ice}_{res,d}$ contribution and justifies the stabilization of adsorption upon d_{XY} enlargement. Again, the coefficient for $E^{w}_{M,d}$ arises from the number of molecules interacting with the surface. Out of the 24 waters in the ensemble, six molecules form a core and another 6 are flat and interact with the metal surface. The mean error value for this model is 2%. A summary of the motif-derived coefficients for all models can be found in Table 4 and its caption. The number of monomers of each type of water

insertion in each model is also displayed for a better clarity of the rationale behind the coefficients.

Table 4: Summary of the prefactors: a, b, c in the general adsorption model for different motifs $E_{ads} = aE^{w}_{M,d} + bE^{ice}_{res,d} + cE_{HB}$ where n_w is the total number of waters; n^{f}_{w} is the number of flat waters in close contact with Oxygen-Metal distance <3 Å (close contact); $n^{f,far}_{w}$ is the number of flat water with Oxygen-Metal distance >3 Å (far contact) and n^{H}_{w} is the number of waters with H-down insertion.

	n_w	n^{f}_{w}	$n^{f,far}_{w}$	n^{H}_{w}	a	b	c
Ice-like	18	9	-	9	0.50	0.67	1
sqrt(37)	26	6	3	17	0.37	0.23	2
Rosette	24	12	-	12	0.50	0.00	2
Lace	18	9	-	9	0.50	0.67	1
sqrt(39)	27	6	3	18	0.33	0.22	2

4.2 Proof of concept: extension to other patterns

The extension of the models to other motifs that can be found on the metal surfaces is a touchstone for the validation of the rationale for the derivation of the structural coefficients. The modeled adsorption energies for other structures than used for parameterization not only needs to be close to the DFT one but the energy ranking between structures has to be maintained. In the following section, different study cases are solved by using Eqs. (1-3) in order to both investigate metastabilities and surface-induced patterning.

Lace structure has been found to be metastable with Rosette for Pd(111) at 0.5 ML coverage,[15] see Figure 5. Since Lace structure deploys a fully surface covering honeycomb-like pattern one would expect that the Ice-like model reproduces its adsorption energy despite its coverage is identical to Rosette. Both models are tested to prove that the DFT-D2 adsorption energy of Lace on Pd(111), -0.626 eV/H_2O, is properly reproduce by Ice-like model with -0.630 eV/H_2O in contrast to Rosette model which deviates further to -0.671 eV/H_2O.

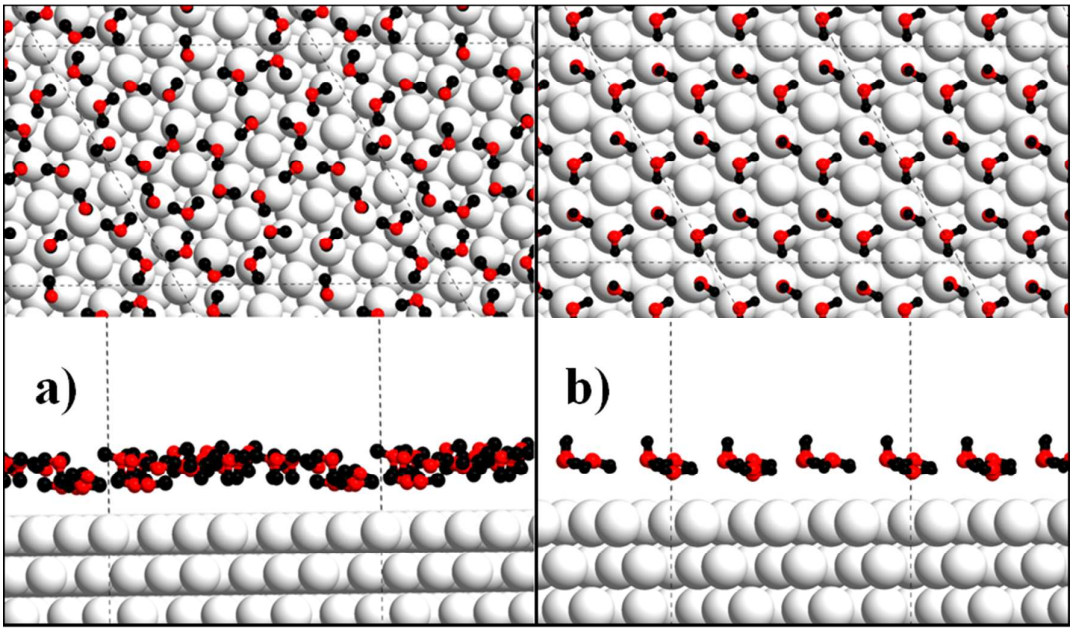

Figure 5: Axial and equatorial views of the lace (a) and H-up Ice-like bilayer (b) structure on Pd(111) surface. Same color code as in Figure 1.

Structural metastability is also found in a more general way for the Ice-like structure where the H-down (Figure 1) and H-up (Figure 5) arrangements may coexist.[31] This umbalance is important with regard water dissociation since a high stability of the H-down arrangement increases the probability of water dissociation in the Ice-like bilayer. Thus, the Ice-like model has to be able to predict the adsorption energy of the H-up ice-like bilayer: following the same rationale employed for the H-down model in Ru(0001) one can deduce that in this case $E_{M,d}^{W}$ should be the average between the flat and H-up insertion (see Table S1 for values) on a water molecule: H-up waters do interact with the metal surface in a similar way that flat inserted waters. The latter was applied to the Ice-like model (Eq. (1)) in order to derive a reliable method to estimate the adsorption energy of H-up Ice-like bilayer on Pt(111) and Pd(111). Pt(111) has been reported to adsorb H-up Ice-like bilayer though in a metastable way with regard to the H-down arrangement that is favored by the van der Waals interaction.[31] The results are plotted in Figure 6 with its numeric expression of in Table 5.

Table 5. DFT-D2 calculated, modeled adsorption energies and relative error for the adsorption of H-up Ice-like bilayer on Pd(111) and Pt(111). All energies are in eV/H_2O.

d_{XY}	Pt(111)			Pd(111)		
	DFT-D2	**Model**	**Error (%)**	**DFT-D2**	**Model**	**Error (%)**
4	-0.569	-0.538	-5.5	-0.612	-0.622	1.7
2	-0.576	-0.547	-5.0	-0.610	-0.628	2.9
0	-0.585	-0.555	-5.1	-0.611	-0.635	4.1
-2	-0.591	-0.563	-4.8	-0.613	-0.641	4.5
-4	-0.591	-0.570	-3.6	-0.616	-0.648	5.2

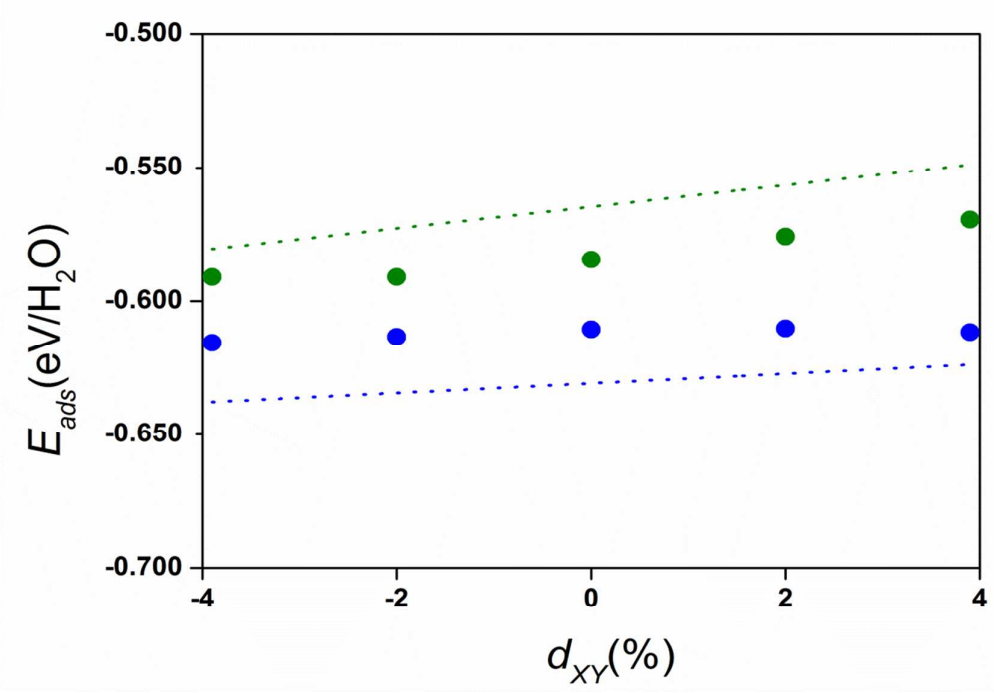

Figure 6: DFT-D2 calculated (colored circles) and modeled (dot line) adsorption energies, E_{ads} eV/H_2O, for H-up Ice-like bilayer at different deformation degrees (±4%) with regard to the equilibrium d_{XY} on Pt(111) (green color) and Pd(111) (blue color).

Surface roughness can alter the energetic preference for a water ensemble thus causing a surface-induced patterning: adsorption on a step of Pt(221) is stabilized by 0.14 eV/H_2O.[32] Provided that steps are common structures in nanoparticles and that the different ensembles have different number of surface interacting waters, the effects that a step adsorption stabilization cause in $E^{w}_{M,d}$ favor Ice-like bilayer (1 in 2 molecules interacts with the surface) over sqrt(37) and Rosette (6 in 26 and 24 molecules respectively). Consequently, the models reproduce the increase in Ice-like bilayer formation with the increase in surface roughness.

4.3 Proof of concept: extension to other metals

Models can also predict relative stability of the studied ensembles on metals where they have not been found which has to be understood as a proof of the predictive power of the models. Figure 7 depicts DFT-D2 and predicted energies of Ice-like bilayer, sqrt(37) and Rosette on Ag, Au, Rh, and Ir (energies in eV/H_2O can be found in Table 6). Thermodynamic trends are reproduced by the models since the DFT-D2

energy (in eV/H_2O) ordering is maintained and so are the relative differences in a truly narrow range. Moreover, despite errors between DFT-D2 and model energies, E_{ads} (eV/H_2O), have different trends it is necessary to bear in mind that the average error magnitude of the model is far below the traditionally used 5% significance error. The sqrt(37) is the most stable of all three ensembles in all cases. Further, water deposition on Ag can be understood as the formation of small clusters like those in the Rosette structures, that are more stable than Ice-like, and close to the sqrt(37). This agrees with the formation of hexameric clusters of flat-lying waters for Ag.[6] On Au structures the same pattern is followed though with more endothermic energies thus explaining the origin of amorphous and labile nature of the aggregates.[33] The larger adsorption of an isolated water molecule found for Ag[5] justifies this difference. The trends found for Rh[34] and Ir(111) are in line with the observation of molecular continuous water layers on both Rh[34] and Ir(111).[35]

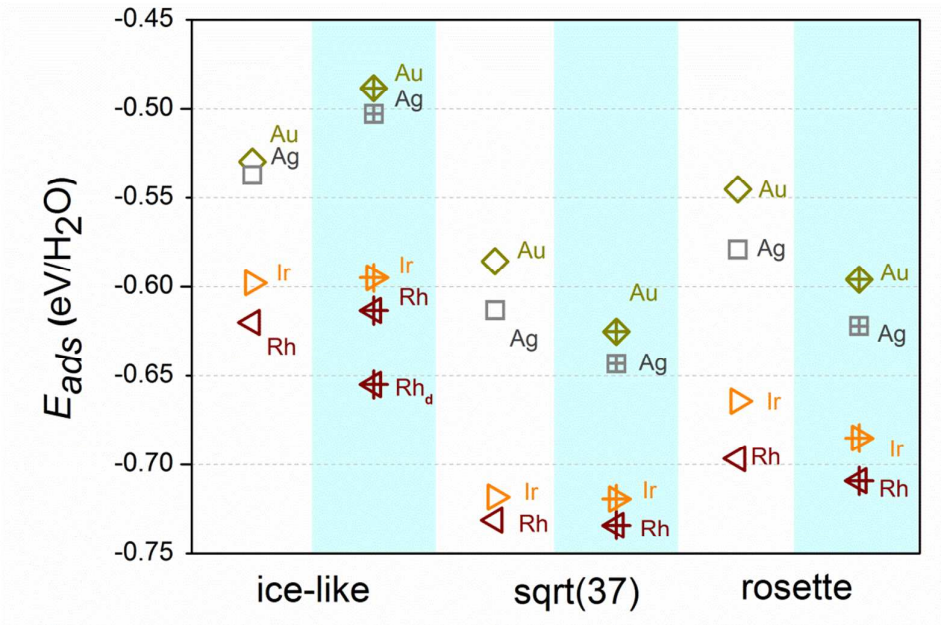

Figure 7: DFT-D2 calculated and modeled (blue background) adsorption energies, E_{ads} H_2O, for ice, sqrt(37), and Rosette for different fcc(111)-surface metals.

Table 6. DFT-D2 calculated, modeled adsorption energies and relative error for the adsorption of different water ensembles on Ir, Rh, Au and Ag(111). All energies are in eV/H_2O.

	DFT-D2			Model				Error (%)		
	Ice-like	**sqrt(37)**	**Rosette**	**Ice-like**	**Ice-like diss.**	**sqrt(37)**	**Rosette**	**Ice-like**	**sqrt(37)**	**Rosette**
Ir(111)	-0.598	-0.718	-0.664	-0.622	N.A.	-0.710	-0.685	4.0	1.2	3.1
Rh(111)	-0.620	-0.730	-0.697	-0.682	-0.655	-0.734	-0.709	10.1	0.5	1.8
Au(111)	-0.529	-0.585	-0.545	-0.516	N.A.	-0.595	-0.554	-2.5	1.6	1.7
Ag(111)	-0.537	-0.613	-0.579	-0.542	N.A.	-0.606	-0.567	0.8	-1.2	2.1

5. Conclusions

Physically meaningful models obtained by decomposing the adsorption energy of water films into basic, easy-to-calculate contributions have been developed for several structures including: Ice-like bilayer, sqrt(37), and clusters (Rosette). The roles of the two leading contributions representing the water-metal and water-water interactions are elucidated by small models. When combined with the coefficients that can be derived from the structures of the motifs, these models provide a valuable estimate for the adsorption energies of different ensembles. The values obtained with the model consistently fit DFT-D2 results: minimum energy structures are properly reproduced on hexagonal close packed planes of Pd, Pt, and Ru as they are predicted, altogether with the energy ranking, for Au, Ag, Rh, and Ir. This approach and modeling justify, in general terms, two kinds of water layer structures. The first type fully covers the surface and is then resonance-dependent. This category can be further divided into hexagonal-only: including H-down and H-up Ice-like, Lace, dissociated Ice-like, and multi-cycle patterned structures with combinations of five, six and seven membered rings like sqrt(37) and sqrt(39). The second group is made by those resonance-independent which do not fully cover the surface like Rosette. Our models should be easily adaptable to any of these families of structures on hexagonal close-packed transition metal surfaces by the evaluation of the coefficients accordingly to the motif.

In summary, we have presented a robust motif-based set of models able to estimate the energies of a wide set of water structures while providing a physical insight of the nature of the interaction, that opens a new path in the study of the wide-spread water-metal interactions.

Acknowledgements

The authors thank the ERC-2010-StG-258406 Bio2chem-d project, MINECO (CTQ2012-33826) and BSC-RES for supporting this work.

References

[1] Carrasco, J.; Hodgson, A.; Michaelides, A. A molecular perspective of water at metal interfaces. Nature Mater. **2012**, 11, 667-674.

[2] Azimi, G.; Dihman, R.; Kwon, H.M.; Paxson, A.T.; Varanasi, K.K. Hydrophobicity of rare-earth oxide ceramics. Nature Mater. **2013**, 12, 315-320.

[3] Haq, S.; Hodgson, A. Water adsorption and the wetting of metal surfaces. Surf. Sci. Rep. **2009**, 64, 381-451.

[4] Tianshu, L.; Donadio, D.; Galli, G. Ice nucleation at the nanoscale probes no man's land of water. Nature Commun. **2013**, 4, 1887.

[5] Michaelides, A.; Ranea, V.A.; de Andres, P.L.; King, D.A. General model for water monomer adsorption on close-packed transition and noble metal surfaces. Phys. Rev. Lett. **2003**, 90, 216102.

[6] Michaelides, A.; Morgenstern, K. Ice nanoclusters at hydrophobic metal surfaces. Nature. **2007**, 6, 597.

[7] Carrasco, J.; Michaelides, A.; Scheffler, M. Insight from first principles into the nature of the bonding between water molecules and 4d metal surfaces. J. Chem. Phys. **2009**, 130, 184707.

[8] Tatarkhanov, M.; Ogletree, D.F.; Rose, F.; Mitsui, T.; Fomin, E.; Maier, S.; Rose, M.; Cerdá, J.I.; Salmeron, M. Metal-and hydrogen-bonding competition during water adsorption on Pd(111) and Ru(0001). J. Am. Chem. Soc. **2009**, 131, 18425-18434.

[9] Schnur, S.; Gross, A. Properties of metal–water interfaces studied from first principles. New J. Phys. **2009,** 11, 125003.

[10] Ortiz-Young, D.; Chiu, H.C.; Kim, S.; Voitchovsky, K.; Riedo, E. Nature Commun.**2013**, 4, 2482.

[11] Mavrikakis, M.; Hammer, B.; Norskov, J.K. Effect of strain on the reactivity of metal surfaces. Phys. Rev. Lett. **1998**, 81, 2819.

[12] Schnur, S.; Gross, A. Strain and coordination effects in the adsorption properties of early transition metals: A density-functional theory study. Phys. Rev. B. **2010**, 81, 033402.

[13] Nie, S.; Feibelman, P.J.; Bartelt, N.C.;Thrümer, K. Pentagons and heptagons in the first water layer on Pt (111). Phys. Rev. Lett. **2010**, 105, 026102.

[14] Ogasawara, H.; Brena, B.; Nordlund, D.; Nyberg, M.; Pelmenschikov, A.; Petterson, L.G.M.; Nilsson, A. Phys. Rev. Lett. **2002**, 89, 276102.

[15] Standop, S.; Morgernstern, M.; Michely, T.; Busse, C. H_2O on Pt(111): structure and stability of the first wetting layer. J. Phys. Condens. Matter. **2012**, 24, 124103.

[16] Cerdá, J.; Bocquet, M-L.; Feibelman, P.J.; Mitsui, T.; Rose, M.; Fomin, E.; Salmeron, M. Novel water overlayer growth on Pd(111) characterized with scanning tunneling microscopy and density functional theory. Phys. Rev. Lett. **2004**, 93, 116101.

[17] Doering, D.L.; Madey, T.E. The adsorption of water on clean and oxygen-dosed Ru (011). Surf. Sci. **1982**, 123, 305.

[18] Feibelman, P.J. Partial dissociation of water on Ru (0001). Science. **2002**, 295, 99.

[19] Kresse, G.; Furthmüller, J. Efficiency of ab-initio total energy calculations for metals and semiconductors using a plane-wave basis set. Comput. Mater. Sci. **1996**, 6, 15.

[20] Blöchl, P.E. Projector augmented-wave method. Phys. Rev. B. **1994,** 50, 17953.

[21] Kresse, G.; Joubert, D. From ultrasoft pseudopotentials to the projector augmented-wave method. Phys. Rev. B. **1999**, 59, 1758.

[22] Perdew, J. P.; Burke, K.; Ernzerhof, K. Generalized gradient approximation made simple. Phys. Rev. Lett. **1996**, **77**, 3865.

[23] Grimme, S. Semiempirical GGA-type density functional constructed with a long-range dispersion correction. J. Comput. Chem. **2006**, 27, 1787.

[24] Bučko, T.; Lebègue, S.; Ángyán, J. G.; Hafner, J. Improved description of the structure of molecular and layered crystals: Ab initio DFT calculations with van der Waals correction. J. Phys. Chem. A. **2010**, 114, 11814.

[25] Ruíz, V.G.; Liu, W.; Zojer, E.; Scheffler, M.; Tkatchenko, A. Density-functional theory with screened van der Waals interactions for the modeling of hybrid inorganic-organic systems. Phys. Rev. Lett. **2012**, 108, 146103.

[26] Weissenrieder, J.; Feibelman, P.J.; Held, G. Experimental evidence for a partially dissociated water bilayer on Ru (0001). Phys. Rev. Lett. **2004**, 93, 196102.

[27] Haq, S.; Clay, C.; Darling, G.R.; Zimbitas, G.; Hodgson, A. Growth of intact water ice on Ru(0001) between 140 and 160 K: Experiment and density-functional theory calculations. Phys. Rev. B. **2006**, 73, 115414.

[28] Andersson, K.; Nikitin, A.; Pettersson, L.G.M.; Nilsson, A.; Ogasawara, H. Water dissociation on Ru(001): an activated process. Phys. Rev. Lett. **2004**, 93, 196101.

[29] Tatarkhanov, M.; Fomin, E.; Salmeron, M.; Andersson, K.; Ogasawara, H.; Pettersson, L.G.M.; Nilsson, A.; Cerdá, J.I. The structure of mixed HO–OH monolayer films on Ru(0001). J. Chem. Phys. **2008**, 129, 154109.

[30] Feibelman, P.J.; Bartelt, N.C.; Nie, S.; Thürmer, K. Pentagons and heptagons in the first water layer on Pt(111). J. Phys. Chem. **2010**, 133, 154703.

[31] Squiros, T.; Haq, S.; Ogasawara, H.; Takahashi, O.; Öström, H.; Andersson, K.; Petterson, L.G.M.; Hodgson, A.; Nilsson, A. Structure of water adsorbed on the open Cu(110) surface: H-up, H-down, or both? Chem. Phys. Lett. **2006**, 429, 415.

[32] Donadio, D.; Ghiringhelli, L.M.; Delle Site, L. Autocatalytic and Cooperatively Stabilized Dissociation of Water on a Stepped Platinum Surface. J. Am. Chem. Soc. **2012,** 134, 19217.

[33] Gawronski, H.; Morgenstern, K.; Rieder, H. Electronic excitation of ice monomers on Au(111) by scanning tunneling microscopy. Eur. Phys. J. D. **2005**, 35, 349.

[34] Beniya, A.; Sakaguchi, T.; Narushima, K, Mukai, Y.; Yamashita, S.; Yoshimoto J.; Yoshinobu, J.J. J. Chem. Phys. **2009**, 130, 034706.

[35] Shavorskiy, A.; Gladys, M.J.; Held, G. Chemical composition and reactivity of water on hexagonal Pt-group metal surfaces. Phys. Chem. Chem. Phys. **2008**, 10, 6150.